Supporting Information for

Interplay between Single and Cooperative H_2 Adsorption in the Saturation of Defect Sites at MgO Nanocubes

Francia Haque, Fabio Finocchi, Stephane Chenot, Jacques Jupille and Slavica Stankic*

Sorbonne Université, CNRS, Institut des NanoSciences de Paris, INSP, F-75005 Paris, France.

Table of Contents

Computational details

General: The calculations were performed using the Quantum Espresso program suite,[1] within the generalized gradient approximation (PBE)[2] to density functional theory (DFT).[3]

We accounted for the interaction between the ionic cores and the valence electrons by ultra-soft pseudopotentials. A cutoff on the plane-wave expansion of the Kohn-Sham orbitals as large as 40 Ry ensures a good convergence for the structural parameters and the vibrational frequencies.

The vibrational modes (frequencies and atomic displacements) were computed through the Density Functional Perturbation Theory (DFPT)[4] in the harmonic approximation. Tests on known molecules (MgH_2 and H_2O) are used as benchmarks in order to align the calculated frequencies on the measured ones.

The stable conformation of the MgH_2 molecule is linear, with 1.709 Å H-Mg bond length, which is overestimated by 0.3% with respect to the value of 1.7033 Å that is deduced from the vibration-rotation spectrum.[5] The antisymmetric (AS) and symmetric (SS) stretching frequencies have been computed at ν_{AS}=1583 and ν_{SS}=1551 cm^{-1}, respectively. The former one agrees very well with the measured ones: ν_{AS} =1589 cm^{-1} and ν_{AS}=1576 cm^{-1} for enclosed MgH_2 in a Ne matrix.[5,6] As the computed H-Mg stretching frequencies are well aligned with the experimental ones in the molecule, we compare them directly to the IR transmission spectra for hydrogenated MgO nanocrystals.

As far as the isolated water molecule is concerned, within our computational scheme we found a 0.974 Å O-H bond length, a 104.4° HOH angle, ν_{AS}=3840 cm^{-1}, ν_{SS}=3730 cm^{-1} and the H-O-H bending mode at ν_B=1570 cm^{-1}. Our computed νAS and νSS are larger by less than 20 cm^{-1} with respect to the all-electron values that were obtained within the same PBE exchange-correlation approximation. Being overestimated by ~2 % with respect to recent experimental values (ν_{AS} =3756 cm^{-1}, ν_{SS} =3657 cm^{-1} and ν_B =1595 cm^{-1}),[7] we rescaled the computed OH stretching frequencies as ν_{OH}=0.975 ν_{OH}DFT, as usually done in this matter.[8] This allows a better comparison with the measured O-H and H-Mg frequencies for the MgO nanopowders after hydrogen adsorption.

MgO slabs with shifted periodic boundary conditions have been constructed in order to simulate hydrogen splitting on surface sites with different coordination numbers on (001) terraces, mono- and diatomic steps parallel to [010] or [100] directions. Other models have been considered, such as MgO(011) surfaces, which show straight neutral ledges along the [100] direction. We did not simulate polar orientations, as they do not represent thermodynamically stable configurations on powders that have been prepared in dry conditions and should not contribute substantially to heterolytic H_2 splitting. We instead considered point defects, such as MgO di-vacancies in variable number NV_{MgO} (NV_{MgO}=1, 2, 3). On MgO(001), the MgO single divacancy is characterized by a very large dipole moment, which is able to dissociate the water molecule[9] and to split H_2, forming O-H and H-Mg complexes.

The slabs are at least 7 atomic (001) layers thick, up to 9 layers in the slabs with diatomic steps. One or two central layers were kept fixed. The void space separating two slabs that are repeated by periodic boundary

conditions is always larger than 12 Å. These choices have been tested to provide H-adsorption energies that are not biased by the slab thickness and the void space.

For each substrate, H atoms were initially placed close to several distinct O and Mg ions, which differ by ion coordination number and kind of site, and their positions optimized through energy minimization until the largest atomic force did not exceed 5 meV/Å. In order to improve the precision of the computed adsorption energies and avoid introducing a surface dipole following H_2 adsorption, the molecules were split on each slab side.

About a hundred distinct adsorption configurations were thus constructed and optimized. In all cases, we checked that the computed H_2 adsorption energies are almost inde-pendent of the specific shifted boundary conditions that have been used. In the limit of very low H_2 coverage – that is, a single H_2 molecule that is split at a given defect – the characteristics of the formed complexes are mostly influenced by the characteristics of the ions to which H^+ and H^- are bound, such as their coordination numbers and bond lengths. At variance, the co-adsorption of several H_2 molecules could be sensitive, in some cases, to the surface conformation around the complexes. For this reason, the simulated configurations where two H_2 molecules are split on each surface of the slab (cooperative adsorption) are restricted to a few combinations of configurations with a single H_2 molecule. No more than two H_2 molecules are dissociated on the slab surfaces.

Free energy of adsorption: Although the H_2 adsorption energies are needed to compare the relative stability of distinct adsorption configurations, they cannot provide a direct link to the experiments, which probe the thermodynamic stability of OH and HMg complexes as a function of the partial H_2 pressure. We thus evaluate the adsorption free energy $\Delta G_{ads}(P,T)$, by means of a few approximations.

First, the dependence on temperature of the free energy difference between the clean slab and the slab with adsorbed H is neglected. This approximation is rather good and the main error comes from the temperature-dependent phonon contribution to the free energy. Although phonons generally represent a substantial part of the absolute free energy, their contribution to the free energy difference upon H adsorption is expected to come from the modes of the H adatoms.

Here comes the second approximation. The six additional modes in the slab after the adsorption of H- and H+ are localized around the adsorption sites because of the proton light mass. We assumed that this additional phonon contribution roughly compensates for the vibrational free energy of the H_2 molecule in the gas phase. A full calculation of the vibrational free energy of the modes implying the H adatoms for specific configurations – H:MgO(011) and H:MgO(015) – within the harmonic approximation, shows that the error made should not

exceed 10 kJ/mol, which is of the same order as that given by the GGA approximation, but of opposite sign. The GGA is indeed known to underestimate the absolute adsorption energy by roughly ~0.05 – 0.1 eV/H atom, as estimated for H_2 adsorption on $(MgO)_6$ clusters through an accurate comparison to quantum chemistry calculations at the CCSD(T) level.[10]

Third, we neglect the contribution from the configuration entropy which, in contrast with the vibrational entropy, stabilizes the products, as the number of available adsorption configurations on the defective surface is expected to be rather high. Moreover, we always neglected nuclear quantum effects in the adsorption/desorption phenomena.

The previous approximations are very similar to those that are usually adopted in ab initio thermodynamics to evaluate the surface energy as a function of the partial pressure of one or more components.[11,12]

The remaining Gibbs free energy comes from the translational and rotational motions of the free H_2 molecule in the gas phase, which have no equivalent in the adsorbed phase.

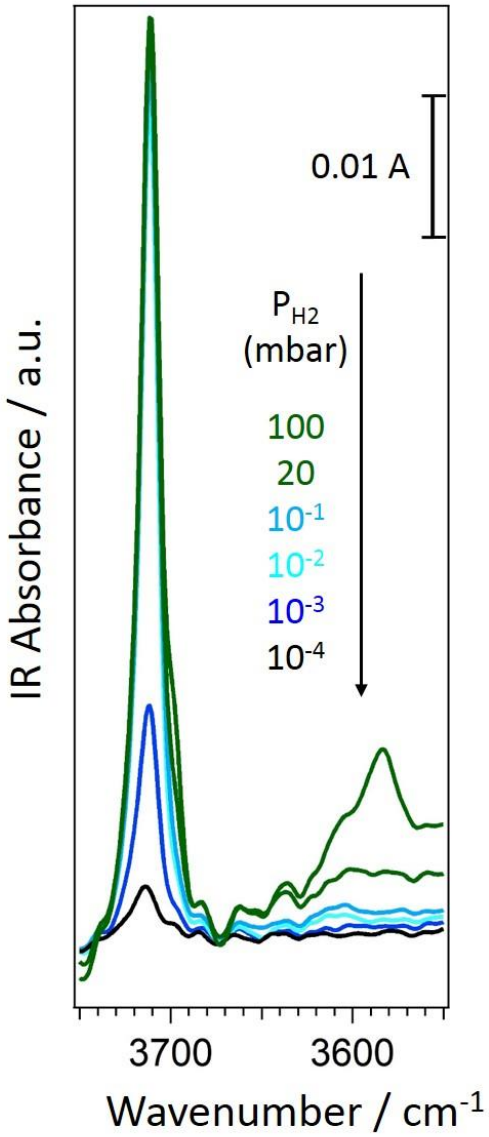

Figure S1. IR spectra of MgO exposed to P_{H2} from 10^{-4} to 100 mbar with a magnified look into the OH stretching vibrations between 3600-3580 cm^{-1}.

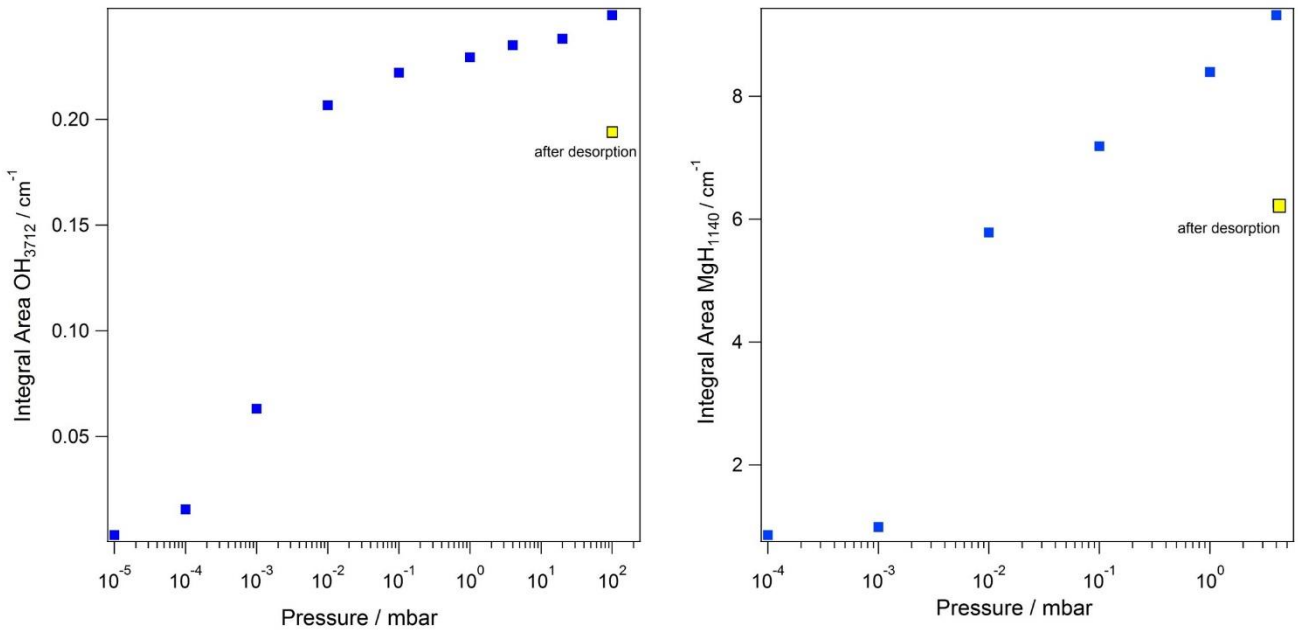

Figure S2. Plot of the integral area vs. H_2 pressure for the IR bands at 3712 cm^{-1} and 1140 cm^{-1}.

References

(1) Giannozzi, P.; Baroni, S.; Bonini, N.; Calandra, M.; Car, R.; Cavazzoni, C.; Ceresoli, D.; Chiarotti, G. L.; Cococcioni, M.; Dabo, I. et al. Quantum Espresso: A Modular and Open-Source Software Project for Quantum Simulations of Materials. *J. Phys. Condens. Matter* **2009**, *21*, 395502.

(2) Perdew, J. P.; Burke, K.; Ernzerhof, M. Generalized Gradient Approximation Made Simple. *Phys. Rev. Lett.* **1996**, *77*, 3865; *Erratum Phys. Rev. Lett.* **1997**, *78*, 1396.

(3) Kohn, W.; Sham, L. J. Self-Consistent Equations Including Exchange and Correlation. *Phys. Rev.* **1965**, *140*, A1133.

(4) Baroni, S.; de Gironcoli, S.; Dal Corso, A.; Giannozzi, P. Phonons and Related Crystal Properties from Density-Functional Perturbation Theory. *Rev. Mod. Phys.* **2001**, *73*, 515.

(5) Shayesteh, A.; Appadoo, D. R. T.; Gordon, I.; Bernath, P. F. The Vibration-Rotation Emission Spectrum of MgH_2. *J. Chem. Phys.* **2003**, *119*, 7785-7788.

(6) Wang, X.; Andrews, L. Infrared Spectra of Magnesium Hydride Molecules, Complexes and Solid Magnesium Dihydride. *J. Phys. Chem. A* **2004**, *108*, 11511-11520.

(7) Tennyson, J.; Bernath, P. F.; Brown, L. R.; Campargue, A.; Csaszar, A. G.; Hodges, J. T.; Naumenko, O. V.; Polyansky, O. L.; Rothman, L. S.; Vandaele, A. C. et al. IUPAC Critical Evaluation of the Rotational-Vibrational Spectra of Water Vapor, Part III: Energy Levels and Transition Wavenumbers for $H_2{}^{16}O$. *J. Quant. Spectr. Rad. Trans.* **2013**, *117*, 29-58.

(8) Cavalleri, M.; Pelmenschikov, A.; Morosi, G.; Gamba, A.; Coluccia, S.; Martra, G. M. Dissociative Adsorption of H_2 on Defect Sites of MgO: A Combined IR Spectroscopic and Quantum Chemical Study. *Studies in Surface Sci Catal.* **2001**, *140*, 131-139.

(9) Ealet, B.; Goniakowski, J.; Finocchi, F. Water Dissociation on a Defective MgO(100) Surface: Role of Divacancies. *Phys. Rev. B* **2004**, *69*, 195413.

(10) Gebhardt, J.; Viñes, F.; Bleiziffer, P.; Hieringer, W.; Görling, A. Hydrogen Storage on Metal Oxide Model Clusters using Density-Functional Methods and Reliable Van der Waals Corrections. *Phys. Chem. Chem. Phys.* **2014**, *16*, 5382-5392.

(11) Zhang, W.; Smith, J. R.; Wang, X.-G. Thermodynamics from Ab Initio Coputations. *Phys. Rev. B* **2004**, *70*, 024103.

(12) Reuter, K.; Stampfl, C.; Scheffler, M. *Handbook of Materials Modeling*, Vol. 1 Fundamental Models and Methods, Sidney Yip (Ed.), Springer (**2005**) ISBN 978-1-4020-3286-8.